DOI: 10.4408/IJEGE.2011-03.B-075

DIRECT MEASUREMENTS OF THE HYDROLOGIC CONDITIONS LEADING UP TO AND DURING POST-FIRE DEBRIS FLOW IN SOUTHERN CALIFORNIA, USA

Jason W. KEAN(*) & Dennis M. STALEY(*)

(*) U.S. Geological Survey, Denver, Colorado, USA

ABSTRACT

Steep, recently burned watersheds can be vulnerable to debris flows. In southern California, USA, the combination of mountainous terrain, dense population, and high fire frequency put new areas at risk to debris flows each year. In an effort to improve predictions of the timing and magnitude of post-fire debris flows, the U.S. Geological Survey (USGS) established five debris-flow monitoring sites in different southern California watersheds burned in 2009. These sites recorded, for the first time, detailed measurements of the hydrologic conditions leading up to and during post-fire debris flows. Measurements included precipitation, hillslope soil-water content, flow stage, and pore pressure. Here, we present initial observations and comparisons of debris flows measured during four storms at our smallest study site (0.01 km^2) located in the Station Fire burn area in the San Gabriel Mountains. The monitored debris flows were generated by progressive entrainment of sediment from hillslope rilling and channel erosion, which occurred in response to short-duration bursts of intense rainfall. The measurements show a distinct change in the flow response over the course of the winter storm season, beginning with a debris-flow dominated response in the first part of the season and followed by more watery flows in the latter part of the season. The change in flow response is presumably related to a decrease in sediment availability.

Key words:*debris flow, fire, monitoring*

INTRODUCTION

In the mountainous western United States, debris flows can be a common hazard after wildfire. In the first one to two years after a fire, most debris flows are generated by surface-water runoff entraining loose material stored on hillslopes and in channels (e.g., Meyer & Wells, 1997; Cannon *et alii*, 2001) and can be triggered by much less rainfall than is required for debris-flow initiation in unburned areas (Cannon *et alii*, 2001; 2008). There is a growing need to better understand these hazards given the high fire frequency associated with recent climate trends (Westerling *et alii* 2006) and continued residential development in steep, fire-prone areas. Rain data, post-event field measurements, and eyewitness accounts have been used to develop both empirical rainfall intensity-duration thresholds for post-fire debris flows (Cannon *et alii*, 2008; Cannon *et alii*, 2010a) and empirical models for debris-flow probability and volume (Cannon *et alii*, 2010b). These tools have proven valuable for assessing post-fire threats over large regions, and, together with weather forecasts, are the foundation for the current southern California debris-flow warning system operated jointly by the National Oceanic and Atmospheric Association (NOAA) and the United States Geological Survey (USGS) (Cannon *et alii*, 2010c; NOAA-USGS Debris Flow Task Force, 2005).

Yet further advancement in predictive capabilities and development of new predictive tools, such as physically based models, requires detailed data on

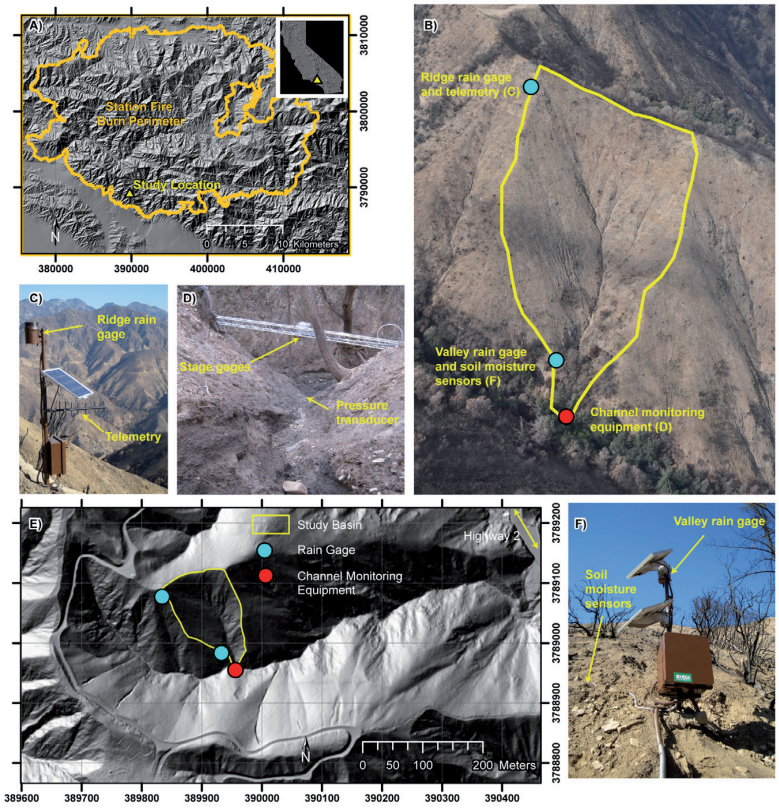

Fig. 1 - Study area. A) Map showing location of study area within the Station Fire burn area. B) Aerial photograph of main study basin taken 11 Feb. 2010. The study area is almost completely denuded of vegetation except at the valley bottom, where a partially burned canopy remains. C) Photograph of ridge station. The rugged terrain in the back ground is typical of the burn area. D) Photograph of channel monitoring equipment near the outlet of the main study area. E) Map of main study basin and drainage area above Highway 2. F) Photograph of valley rain gage and soil moisture probes

the hydrologic conditions leading up to and during post-fire events (e.g. combined time-series of rain and flow stage). Unfortunately, the existence of such data is limited. Limits are imposed by both the destructive nature of flash floods and debris flows, and the very narrow time window available to collect such data. In southern California, the end of the fire season generally corresponds to the beginning of the winter storm season. Installation of a field monitoring network between the fire and the first rainstorm is technically and logistically very difficult. For this reason, available time-series of post-fire runoff is usually restricted to floods, such as those measured at pre-existing stream-flow gauging stations on high-order tributaries. Information on the timing of debris flow is usually only available from rare eyewitness accounts. The lack of timing and other hydrologic information in the low-order channels where debris flows originate has made it difficult to quantify precisely the triggering conditions and mechanics of post-fire debris flows.

In an attempt to bridge the data gap, we have started a program to collect the basic measurements necessary for development and rigorous testing of predictive models of post-fire debris-flow initiation. This type of data will also make it possible to make detailed comparisons between post-fire debris flows and non-fire-related debris flows. The approach involves establishing post-fire debris-flow monitoring stations having some of the measurement capabilities found in long-term debris-flow monitoring sites in unburned areas (e.g. Berti *et alii*, 2000; Marchi *et alii*, 2002; McArdell *et alii*, 2007; Suwa *et alii*, 2009; McCoy *et alii*, 2010). Measurements include precipitation, hillslope soil water-content, flow stage, pore pressure, video, and, at some sites, high-resolution topography from terrestrial and airborne

laser scanning. Each year one to five sites are established in new fires in southern California.

Southern California is an ideal region to conduct this work because of the regular occurrence of large fires (typically three or more each year), variety of geologic settings, predictable winter rainy season; and, more importantly, it is the region of the USA most at risk to these destructive events. Sites are established in small, steep drainage areas (0.01 to 1 km2) as soon as possible after the fire is extinguished (typically late fall). The sites are maintained usually for one or two rainy seasons and then the equipment is moved to more vulnerable locations in new burned areas. The monitoring sites are relocated because rapid post-fire growth of vegetation quickly reduces the debris-flow hazard after one or two years. Following this approach, it is possible over the course of a few years to procure flash-flood and debris-flow data sets in a number of basins of different scales and geologic and topographic characteristics.

The purpose of this paper is to describe our post-fire debris flow monitoring approach in general, present initial results from the first (to our knowledge) direct measurements of post-fire debris flows, and discuss the implications of these results for debris-flow warning systems. Results are presented from the smallest of five post-fire monitoring sites established in 2009. We focus on a comparison of flows measured during a series of four debris-flow producing storms that occurred in the first winter rainy season after the fire.

STUDY SITE

A map of the study site (Arroyo Seco) is shown in Figure 1, and a summary of basin characteristics is given in Tab. 1. The 0.01 km^2 study area is located on the San Gabriel mountain front and drains to the heavily travelled Angeles Crest Highway (Highway 2). The study basin is very steep and composed of soils derived from granitic rocks (Yerkes & Campbell, 2005). Soil thickness ranges from 0.05 cm to about 50 cm. The climate is Mediterranean, and characterized by hot, dry summers and a winter with occasional storms. The native vegetation is chaparral, which is adapted for growing in fire-prone areas. Our instruments are in the same basin as additional equipment for monitoring hillslope hydrology, which is described in Schmidt *et alii* (this volume).

Basin area (km^2)	0.0135
Max./Min. elevation (m)	1040/940
Relief ratio (m/m)	0.72
Mean/Max. slope (degrees)	39/57
Channel slope at station (degrees)	20

Tab. 1 - Topographic characteristics of study area from a 2-m DEM

The study site was burned in the 650 km^2 Station Fire of August and September 2009 - the largest fire in Los Angeles county history. Ninety-nine percent of the study area was burned at moderate to high severity (Station Fire BAER Team, 2009). Several episodes of damaging post-fire debris flows have occurred over the last hundred years in the vicinity of the study site. Eaton (1936) documented post-fire debris flows in the area between 1914 and 1935; the largest of these killed 30 people and damaged 483 homes in the communities of La Crescenta and Montrose (see also, Chawner, 1934). In 1969 and 1978, debris flows following wildfires earlier in the summer caused extensive damage again in the area (Scott, 1971; McPhee, 1989; Shuriman & Slossen, 1992). Debris flows in the winter months following the 2009 Station Fire damaged or destroyed 41 homes along the mountain front (Kim *et alii*, 2010) and caused major damage to a heavily travelled road below the monitoring site.

METHODS

Field reconnaissance for site selection began on 17 Sept. prior to containment on 16 Oct. 2009. The Arroyo Seco site was the second of four sites to be established in the Station Fire (A fifth was established in the 2009 Jesusita Fire in Santa Barbara, California). Installation took place 7-10 Nov. by the authors. The first debris flow occurred 12 Nov. - two days after installation. This short 2-month timeline for site selection and installation highlights one of the principal challenges of post-fire debris-flow monitoring. Photos and specifications of the monitoring equipment at the main station are shown in Fig. 1 and listed in Tab. 2. Similar equipment and sensor configurations were used at our other 2009 monitoring sites. The equipment consists of sensors to measure stage (*H*), pore pressure (*P*), rainfall (*R*), and soil-water content. Stage and pore pressure sensors were located at a cross section 3-m upstream of the confluence with

Measurement	Make and model	Sampling rate	Accuracy ; resolution
Stage (laser)	SICK DT50-HI	10 Hz	±7 mm ; 1 mm
Stage (radar)	Endress+Hauser M FMR250	1 min	±3 mm ; 1 mm
Pore pressure	Campbell Scientific CS450	2 sec	±5 mm ; 1 mm (water depth)
Rain	Texas Electronics TR525	2 sec	±1% ; 0.2 mm
Soil moisture	Decagon EC-5	1 min	±3% ; 0.001 m^3/m^3

*Any use of trade, product, or firm names is for descriptive purposes only and does not imply endorsement by the U.S.Government.

*Tab. 2 - Sensor specifications**

a higher order tributary. Stage was measured using both laser and radar distance meters that were suspended approximately 2-m above the channel on a portable 6-m aluminium bridge. The laser distance meter, which produces an analogue 4-20 milli-Amp signal, was used as the primary stage sensor. The radar distance meter, which could not be sampled as frequently, was used to provide a periodic check on the laser measurement. The two measurements of stage were found to be in reasonable agreement (within 5 cm) for both debris flows and water-dominated flows. Discrepancies between the two sensors were due primarily to different sampling footprints (~3-mm diameter for the laser versus an 8 degree cone for the radar, which, at 2-m above the bed, corresponds to a 28-cm diameter footprint). The datum for the stage gages was taken to be the level of a vented pore-pressure sensor that was cemented into the bedrock beneath the stage gages. After installation, the sensor was buried with 48 cm of sediment to the original bed level.

The stage and pore-pressure sensors, which were located in the partially burned valley bottom, were connected via cables to a data logger and power supply situated 50 m above the channel on the unvegetated hillslope (Fig. 1). A tipping-bucket rain gage and two soil-moisture probes were installed at the data logger site. The soil-moisture probes were buried 5-cm deep on a 20 degree section of hillslope. The laser, pore pressure, and rain gages were sampled at high rates only during rain events (Tab. 2). The soil-moisture and radar sensors were sampled continuously at 1-min. intervals. A second tipping-bucket rain gage was installed near the ridge of the study basin. The ridge rain gage often (but not always) measured less rainfall than the valley rain gage. This difference may have been related to systematically higher wind velocities at the ridge, which would decrease the amount of rain intercepted by the gage. For this reason, only data from the lower (valley) rain gage is used in this paper.

Near-real-time data telemetry was established to check for problems with the sensors and provide a rapid (albeit lower-resolution) assessment of flow conditions. A cell-phone modem located at the ridge site was used to transmit one-minute data from all of the sensors. Higher resolution data from the laser and pore-pressure sensor was downloaded manually due to the large file sizes. Data from the valley datalogger, which did not have cell phone reception, was first relayed to the ridge site via radio and then transmitted to our office computer in Golden, Colorado. Data was collected every 5 min., graphed, and then posted on a public web page (see, for example http://landslides.usgs.gov/monitoring/). The web-page data typically lagged the current conditions by 5-10 min. The 10-Hz laser stage data was processed using a simple median filter with a window size of 5 data points (0.5 sec.). The filter replaces each data point with the median of neighbouring points contained in the window. This filter preserved most of the complex structure of the time series, but removed anomalously high and low readings, such as those caused by missed laser returns and returns from large splashes. At selected 20-min. segments of the stage records, the local variability of the flow was assessed by computing the standard deviation (σ) of the stage data about a smoothed version of the time series (H_{smooth}). This was done by smoothing the median-filtered signal using a 21-point moving (box-car) average (2-second time window), subtracting it from the unsmoothed series (H), and calculating the standard deviation of the residuals. For a for a 20-min. time window, σ is computed from 6000 residuals of $H - H_{smooth}$.

Continuous time series of rainfall intensities for different durations (D = 2, 5, 10, 15, 30, 60, 180, 360, and 720 min.) were calculated from the rainfall data. The rainfall intensity, I, for a given duration was calculated at 1-min. intervals by first taking a backward difference of the cumulative rainfall at the current time and D minutes earlier; and then dividing this difference by the duration. Results for the 10- and 60- min. intensities (I_{10} and I_{60}) are presented here. The 10-min. duration was chosen, because a correlation analysis of stage and rain intensities from all five 2009 monitoring sites showed I_{10} to have the highest cross-correlation with stage. The 60-min. duration was chosen for comparison

because it is used more commonly in the post-fire literature. Field visits to the site were made following each storm to download data, check instruments, and document the geomorphic response. The latter was done by hiking the channel between its intersection with Highway 2 and the main study site. Evidence of debris-flow deposits were noted along the way. In many areas, including at the instrumented cross-sections, debris-flow deposits were not preserved because the adjacent banks were too steep/confined to support a deposit and/or the deposits were washed away by subsequent more watery flows.

RESULTS AND DISCUSSION

Four storms produced debris flows at or downstream of the monitoring site. The first was a localized thunderstorm that occurred on 12 Nov. 2009. The hillslope response to this storm is discussed in detail in Schmidt *et alii* (this volume). The last three were extensive frontal storms that occurred on 12 Dec. 2009, 18 Jan. 2010, and 6 Feb. 2010. All storms caused at least temporary closure of Highway 2. At the time of this writing (Jul. 2010) the highway remains closed due to damage from the 6 Feb. 2010 event. Time series plots of data from each storm are shown in Fig. 2-5. Each figure contains multiple panels with time in Pacific Standard Time. The first two panels (A and B) show long-duration time windows of rain, stage, and pore pressure data. The last panels (C-E) show details of stage data for selected short-duration time windows together with the value of σ during that time.

RAINFALL

Time series of 10- and 60-min. intensities for the two storms are shown in panel A of Fig. 2-5. Cumulative rainfall from the start of the storm is shown with the dotted lines in the B panels. In almost all cases, distinct periods of flow, which are characterized by clusters of peaks in flow stage or pore pressure, occur within a few minutes of a local peak in the 10-min. intensity. In contrast, the much broader peaks in 60-min. intensities typically lag peaks in flow activity by 10 min. or longer. The em-

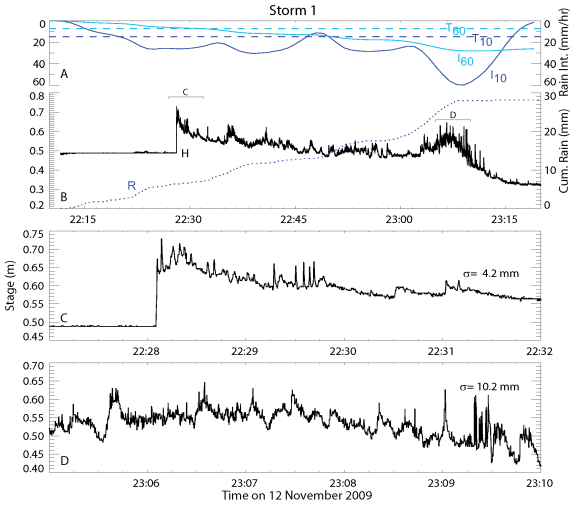

Fig. 2 - Sensor data for Storm 1 (12 Nov. 2009). (A) I_{10} and I_{60} (solid dark and light blue, respectively), and corresponding rainfall intensity-duration thresholds from Cannon et alii (2008) (T_{10}, dotted dark blue line; T_{60}, dashed light blue line). (B) Stage (H), and storm cumulative rainfall (R, dotted blue) for 70 min. The datum for stage and pressure head is the level of the pressure transducer. Flow periods beneath brackets "C" and "D" are shown in detail in the next panels. (C-D) Stage during 5-min. time windows. The stage scale is 0.3 m. The standard deviation (σ) of the data about a 2-sec. running average is given for each 5-min. time window

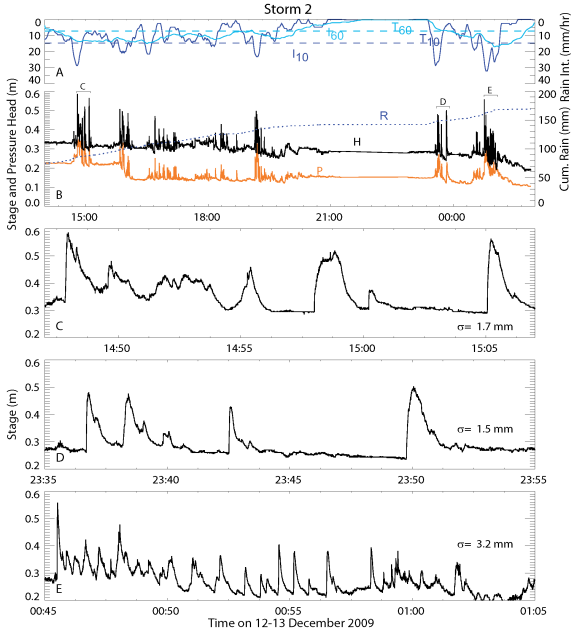

Fig. 3 - Sensor data for Storm 2 (12 Dec. 2009). (A) See caption Fig. 2A. (B) Stage (H), pore pressure head (P, orange line), and storm cumulative rainfall (R, dotted blue) for 12 hrs. (C-D) Stage and σ during 20-min. time windows. The stage scale is 0.4 m

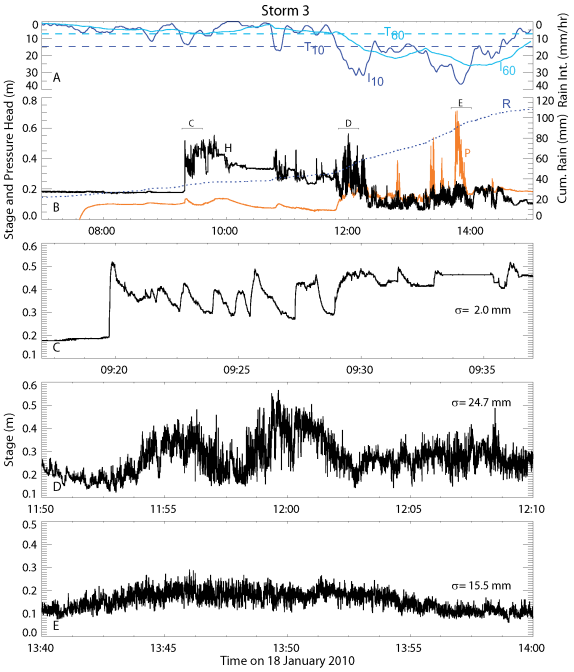

Fig. 4 - Sensor data for Storm 3 (18 Jan. 2010). Notation and time scales same as Fig. 3. The stage scale in (C-E) is 0.5 m

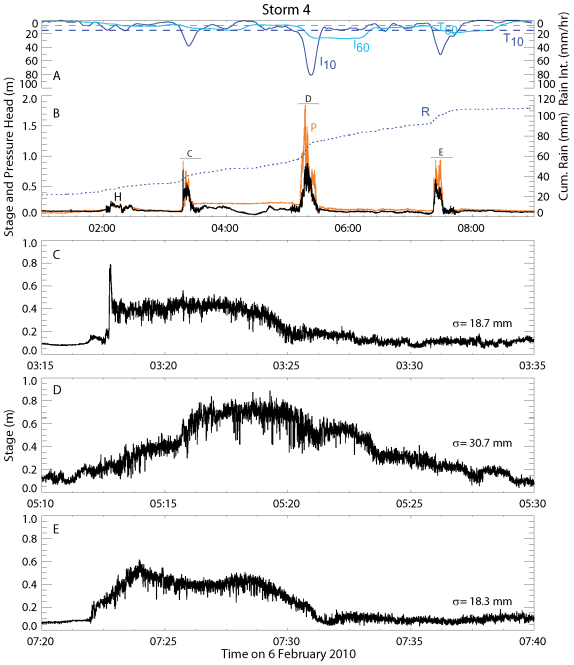

Fig. 5 - Sensor data for Storm 4 (6 Feb. 2010). Notation and time scales same as Fig. 3. The stage scale in (C-E) is 1 m

pirical rainfall-intensity duration thresholds of CANNON *et alii* (2008) are shown in the A panels of Fig. 2-5 for comparison. These thresholds, which were developed for this area prior to this study, are defined by the equation $I = 7.2\ D^{-0.4}$.

STAGE

The plots of stage shown in Fig. 2-5 show a complex and evolving flow response. The first storm on 12 Nov. 2009 lasted 1 hour (Fig. 2). Flow began abruptly at 22:28, a few minutes after a local peak in I_{10} and only 15 min. after the onset of rain. The flow front (Fig. 2C) had the distinct asymmetric shape characteristic of debris-flow surges. This shape is caused by a longitudinal non-iformity in resisting stresses, which is produced by the hintergranular friction of coarser grains at the front followed by lowerore watery recessional flow (HUNGR, 2000). Although debris-flow deposits were observed downstream of the station, no evidence of debris-flow deposits was found at the station. It is unlikely, however, that levees could be preserved at that levees could be preserved at that location as steep banks confined flow and precluded deposition. Also, intense rain at the end of the storm could have washed away evidence of thin mud deposits. Stage and video data of surges recorded at a nearby monitoring site during a different storm provide indirect support of our conclusion that the surge shown in Fig. 2C is a small debris flow. This data had surges of similar shape and video confirmed the flows were debris flows with large clasts in the front followed by water-rich recessional flows. Towards the end of the storm, a brief high intensity burst of rain (I_{10} = 60 mm/hr) produced a second major pulse of flow (Fig. 2D). This flow peak was more symmetrical than the initial surge. It also had greater variability in stage: the value of σ increased from 4.2 mm during the initial surge to 10.2 mm during the second pulse (Fig. 2C and 2D). The increase in σ is likely the result of an increase in the percentage of water in the flow, which tends to produce a more agitated flow surface with larger, high frequency (> 0.5 Hz) stage fluctuations.

Stage measurements from the second storm on 12 Dec. 2009 are shown in Fig. 3. This storm contains seven major periods of flow, the first of which begins at 14:48. Within each period of flow there are 4 to 30 steep-fronted surges that range in height from 5 to 25 cm (Fig. 3 C, D, and E). Flow periods between those highlighted in Fig. 3C and 3D, which are not shown in detail for space considerations, have similar surge frequency and σ characteristics as the C and D periods. In contrast, the last flow period (Fig. 2E) has a distinctly higher average surge frequency (35 seconds apart versus 220 seconds apart). This set of surges comes during the most intense rain of the storm. Possible reasons for the increase in surge frequency near the end of the storm include: existence of a more well-developed drainage network, a potential increase in the number of active overland flow pathways on the hillslopes as a result of the higher rain intensity, and/or greater flow velocities due to increased water content. Additional insight into this phenomenon may be gained by analysis of infiltration data and pre- and post-event terrestrial LiDAR surveys, which is currently underway.

The third storm on 18 Jan. 2010 (Fig. 4) also contained multiple periods of flow, three of which are shown in detail in Fig. 4C, D, and E. The first surges (Fig. 4C) began at 9:20 and had similar characteristics to the ones on 12-13 Dec. 2009. At approximately 11:50 the character of the flow changes substantially (Fig. 4D), and the value of σ increased an order of magnitude from 2 mm to 25 mm (Fig. 4D). The flow in this time period is no longer characterized by well-defined surges, but rather by high-frequency fluctuations about roughly symmetric, lower-frequency trends in stage. Later in the storm (Fig. 4E), the flow has similar high-frequency fluctuations about a near steady flow. The change in flow characteristics is likely due to a transition from debris flow to more water-dominated flow, as a result of a change in hillslope and channel sediment supply. This conclusion is supported by field observations after the 18 Jan. 2010 storm, which showed that large portions of the main channel and many rills upstream of the site were scoured to bedrock.

Stage data from the fourth storm on 6 Feb. 2010, is shown in Fig. 5. This storm had the highest recorded rain intensities of the season and produced three major periods of flow, which are shown in detail in Figs. 5c-e. The first flow period began at 3:17 with a distinct 0.8 m high debris-flow front (Fig. 5c). The flow immediately following this front, as well as the flows during the two later bursts of rain (Figs. 5 d-e), have σ characteristics similar to the more watery flows of the latter half of the 18 Jan. 2010 storm. This similarity suggests that the water content of the flows during the 6 Feb. 2010 storm was relatively high and further support our hypothesis that the transition in primary flow response midway through the 18 Jan. 2010 storm is related to sediment supply. However, despite the fact the three flow periods during the 6 Feb. 2010 storm have the rapid stage fluctuations characteristic of high water content flows, it is not possible from the stage records alone to identify whether the flows after the initial 3:17 surge are water floods, hyper-concentrated flows, or debris flows. Post-event field observations of debris-flow deposits downstream of the site and major debris-flow damage to Highway 2 suggest that the measured last two pulses of flow (Fig 5d and 5e) either were debris flows or developed into debris flows downstream of the site. In fact, the regional debris-flow response during this storm was the largest of the season and damaged or destroyed 41 homes (Kim *et alii*, 2010). The most common characteristic shared by the plots in Fig. 2-5 is the close timing between flow periods and local peaks in 10-min. rainfall intensity. This connection provides strong evidence that the debris flows in the main study area were initiated by surface-water runoff rather than by landslide failure by infiltration processes, which operate typically on longer time scales. This conclusion is supported by post-event field observations, which documented extensive rilling on hillslopes (Fig. 6), substantial channel erosion (Fig. 7), and the absence of new landslide scars.

Fig. 6 - Photograph of hillslope erosion after the 12 Nov. 2009 storm (Storm 1). The largest burned shrub in the photo is about 3-m high

Fig. 7 - Photograph of channel erosion after the 18 Jan. 2010 storm (Storm 3). Geologist for scale in center of photo. Much of the channel bed in the foreground is bedrock

PORE PRESSURE

Measurements of pore pressure head (m of water depth) are shown in panel B of Fig. 3-5. No pore pressure changes were detected during the first short storm on 12 Nov. 2009. Throughout the entire second storm on 12 Dec. 2009 the pore pressure sensor is buried beneath at least 20 cm of sediment. At the time of the first surge at 14:48 the pore pressure sensor indicates the water table is about 3 cm below the bed surface. After the first surge, pore pressure generally tracked changes in flow stage; however, the pressure response was muted throughout the entire event, because the bed was not completely saturated. McCoy *et alii* (2010; this volume) observed similar responses during debris flows measured at the Chalk Cliffs monitoring site. Unsaturated bed conditions also were present during the third storm on 18 Jan. 2010 up until about 11:50 (Fig. 3b). The bed nearly reached saturation at 8:00 after about 25 mm of rainfall, as can be seen by the close agreement between the stage and pressure head. The muted signal of the pore pressure during the first several sets of surges (9:20 to 11:50) indicates the bed did not reach complete saturation until about 11:50. At this time there is a rapid increase in pressure that eventually becomes greater than hydrostatic.

The transition of the pressure signal around 12:00 on 18 Jan. 2010 from less than hydrostatic to greater than hydrostatic is probably associated with erosion of the bed material above the sensor, which at least removed the unsaturated layer that previously damped the signal. After about 12:10, the pore pressure head remains consistently above the stage and has occasional spikes that are several times hydrostatic. Excess pore pressures have been observed during both field (McArdell *et alii*, 2007; McCoy *et alii*, 2010) and large-scale experimental debris flows (Iverson *et alii*, 2010). However, given the stage characteristics of the flow during this time (e.g. Fig. 4E), which are not characteristic of debris flow, it is more likely that the non-hydrostatic pressures measured here are caused by accelerating water-dominated flow. Non-hydrostatic conditions in water flows are common in steep irregular channels, such as the one at the station (Denlinger & O'Connell, 2008). The fact that the spikes in pressure often coincide with local peaks in I_{10} suggests the discharge during these times was very high; the fact that the stage also was low implies the flow velocity was very fast. Similar high pore pressures were observed during the 6 Feb. 2010 event (Fig. 5).

IMPLICATIONS FOR WARNING AND MODELLING

The rapid response to rainfall in the 0.01 km^2 basins show that real-time data from post-fire debris-flow monitoring stations cannot provide sufficient warning of impending debris flows and floods for communities downstream. Instead, warnings with practical lead times of several hours must come from a combination of weather forecasts, rainfall measurements of approaching storms, and debris-flow triggering thresholds, such as a rainfall-intensity duration threshold used in the current southern California debris-flow warning system. In addition, the transition of the dominant flow from debris flow to flood, which occurred during the 18 Jan. 2010 storm under similar rain conditions, demonstrates the difficulty of differentiating warnings for debris flows from those for floods.

A comparison of rainfall thresholds developed by Cannon *et alii* (2008) with the data in Fig. 2-5, show that measured rainfall intensities exceeded the thresholds during most of major flow periods. Although rain data collected at the 2009 monitoring sites was used to slightly refine these thresholds (adjusting the thresholds upwards by 6 percent, Cannon *et alii*, 2010a), it is unlikely availability of additional data

would produce major revisions to the current thresholds. Despite the fact that the current regional rain thresholds are about as good as they can be, additional data, such as that presented here, may help define alternative basin-specific debris-flow triggering conditions (e.g. extent and magnitude of surface water runoff), which could be implemented in a warning system. In the meantime, this data, together with the data from the other four monitoring sites, shows that closer attention should be paid to short duration rain intensities (e.g. 10 min.), which are connected most closely to the events, but have received less attention in the post-fire literature than longer durations (see review in Cannon *et alii*, 2008). This also increases the importance of rainfall monitoring "upwind" of the burn area, which can verify high intensity cells in advancing storms before they are over the burn area.

In regards to modelling, the high correlation between short-duration high-intensity rainfall and debris flows suggests that a simple rainfall runoff model may be a useful tool to predict the timing of post-fire flash flood and debris-flow from low-order basins. However, without the addition of physically based models for initiation (i.e. how surface-water flow becomes debris flow), entrainment, and routing, such models will not reproduce the complex stage changes of the debris-flow surges shown in Fig. 2-5, nor predict accurately the peak stage of debris flows, which are likely to be much higher than flood peaks (Hungr, 2000).

SUMMARY AND CONCLUSIONS

This paper has presented initial results from the first post-fire debris flows to be recorded by in-situ monitoring equipment. The flows were generated by surface-water runoff, and the timing of flows corresponded most strongly with short duration (~10-min.) bursts of rain. High frequency (10 Hz) stage data from a laser distance meter with a small beam footprint was used to provide a qualitative measure of the water content of the flows. The addition of normal stress sensors and video cameras at future monitoring sites may permit determination of flow-density time series that could better distinguish the flow response (debris flow, hyper-concentrated flow, water flood). Approximately halfway through the third winter storm of the season, the primary flow response in the small, 0.01 km^2 basin transitioned abruptly from debris flow to more water-dominated flow, and this transition is likely related to a decrease in the sediment availability in the hillslopes and channels. Continued post-fire debris-flow monitoring of this type should provide detailed documentation of the varied flow responses that can occur in post-fire settings, and this, in turn, will help improve predictions of post-fire debris flows.

ACKNOWLEDGEMENTS

Land access was granted by the City of Pasadena. Robert Leeper provided field assistance. Helpful reviews by Sue Cannon, Scott McCoy, and Kevin Schmidt greatly improved the manuscript.

REFERENCES

Berti M., Genovois R., LaHusen R., Simoni A., & Tecca P.R. (2000) -*Debris flow monitoring in the Acquabona watershed on the Dolomites (Italian Alps)*, Physics and Chemistry of the Earth, Part B : Hydrology, Oceans and Atmosphere, **25**: 707-715, doi: 10.1016/S1464-1909(00)00090-3.

Cannon S.H., Kirkham R.M., & Parise M. (2001) - *Wildfire-related debris-flow initiation processes, Storm King Mountain, Colorado*, Geomorphology, **39**: 171-188.

Cannon S.H., Gartner J.E., Wilson R.C., Bowers J.C., & Laber J.L. (2008) -*Storm rainfall conditions for floods and debris flows from recently burned areas in southwestern Colorado and southern California,* Geomorphology, **96**: 3-4, 250-269.

Cannon S.H., Boldt E.M., Kean J.W., Laber J.L., & Staley D.M. (2010a) - *Relations between rainfall and postfire debris-flow and flood magnitudes for emergency-response planning, San Gabriel Mountains, southern California: U.S.* Geological Survey Open File Report 2010-1039, 31 pp.

Cannon S.H., Gartner J.E., Rupert M.G., Michael J.A., Rea A. H., & Parrett C. (2010b) -*Predicting the probability and volume of postwildfire debris flows in the intermountain western United States*, GSA Bulletin, **122**: 1/2,127-144, doi: 10.1130/B26459.1.

Cannon S.H., Gartner J.E., Rupert M.G., Michael J.A., Staley D.M., & Worstell B.B. (2010c) - *Emergency assessment of postfire debris-flow hazards for the 2009 Station fire, San Gabriel Mountains, southern California: U.S.* Geological Survey Open-File Report 2009-1227, 27 pp.

Chawner W.D. (1934) - *The Montrose-La Crescenta (California) flood of January 1, 1934, and its sedimentary aspects*, California Institute of Technology, Master's thesis, 78 pp.

Denlinger R.P. & O'Connell D.R.H (2008) - *Computing nonhydrostatic shallow-water flow over steep terrain*, Journal of Hydraulic Engineering, **134**: 11, 1590-1602.

Eaton E.C. (1936) - *Flood and erosion control problems and their solution,* Proceedings of the American Society of Civil Engineers, **62**: 8, 1302-1362.

Hungr O. (2000) - *Analysis of debris flow surges using the theory of uniformly progressive flow*, Earth Surface Processes and Landforms, **25**: 483-495.

Iverson R. M., Logan M., LaHusen R.G., & Berti M. (2010) - *The perfect debris flow? Aggregated results from 28 large-scale experiments,* Journal of Geophysical Research, **115**: F03005, doi:10.1029/2009JF001514.

Kim V., Vives R., Rong-Gong L., & Gottlieb J. (2010) - *Mandatory evacuations ordered for 500 homes in La Canada Flintridge, La Crescenta and Acton*, Los Angeles Times, 6 February 2010.

Marchi L., Arattano M., & Deganutti A. (2002) - *Ten years of debris-flow monitoring in the Moscardaro Torrent (Italian Alps),* Geomorphology, **46**: 1-17, doi: 10.1016/S0169-555X(01)00162-3.

McArdell B.W., Bartelt P., & Kowalski J. (2007) - *Field observations of basal forces and fluid pore pressure in debris flow*, Geophysical Research Letters, **34**: L07406, doi: 10.1023/A:1008064220727.

McCoy S.W., Kean J.W., Coe J.A., Staley D.M., Wasklewicz T.A., & Tucker G.E. (2010) - *Evolution of a natural debris flow: In situ measurements of flow dynamics, video imagery, and terrestrial laser scanning*, Geology, **38**-8: 735-738, doi: 10.1130/G30928.1.

McCoy S.W., Coe J.A., Kean J.W., Tucker G.E., Staley D.M., & Wasklewicz T.A. (This volume) - *Observations of debris flows at Chalk Cliffs, Colorado, USA: Part 1*, In-situ measurements of flow dynamics, tracer particle movement and video imagery from the summer of 2009.

McPhee, J.A. (1989) - *The Control of Nature*, Farrar, Straus and Giroux, New York, 272 pp.

Meyer G.A., & Wells S.G. (1997) - *Fire-related sedimentation events on alluvial fans, Yellowstone National Park, U.S.A.*, Journal of Sedimentary Research, **67**(5): 776-791.

NOAA-USGS Debris Flow Task Force (2005) - *NOAA-USGS debris-flow warning system - Final report: U.S.* Geological Survey Circular **1283**: 47 pp.

Schmidt, K.M., Hanshaw M.N., Howle J.F., Kean J.W., Staley D.M., Stock J.D., Bawden G.W. (This volume) - *Hydrologic conditions and terrestrial laser scanning of post-fire debris flows in the San Gabriel Mountains, CA, USA*.

Scott, K.M. (1971) - *Origin and sedimentology of 1969 debris flows near Glendora, California, U.S.* Geological Survey Professional Paper **750**-C: C242-C247.

Shuriman G., & Slossen J.E. (1992) - *Forensic engineering - Environmental case histories for civil engineers and geologists*, chap 8, Academic Press, Harcourt Brace Javanovich, San Diego, p. 168-209.

Station Fire BAER Team (2009) - *Station Fire Burned Area Emergency Response (BAER) Report,* FS-2500-8, U.S. Forest Service, 22 pp.

Suwa H., Okano K., & Kanno T. (2009) - *Behavior of debris flows monitored on test slopes of Kamikamihorizawa Creek, Mount Yakedake, Japan,* International Journal of Erosion Control Engineering, **2-2**: 33-45.

Westerling A.L., Hidalgo H.G., Cayan D.R. & Swetnam T.W. (2006) - *Warming and earlier spring increase western U.S. forest wildfire activity*, Science, **313**: 940-943., doi: 10.1126/science.1128834.

Yerkes R.F., & Campbell R.H. (2005) - *Preliminary geologic map of the Los Angelse 30'x60' Quadrangle, Southern California, U.S.* Geological Survey Open-file Report 2005-1019.